Available online at www.sciencedirect.com
SCIENCE DIRECT
Journal of Catalysis 232 (2005) 117–126
JOURNAL OF CATALYSIS
www.elsevier.com/locate/jcat

Activation of hydrogen peroxide in copper(II)/amino acid/H_2O_2 systems: effects of pH and copper speciation

Tsai-Yin Lin, Chien-Hou Wu *

Environmental Chemistry Laboratory, Department of Atomic Science, National Tsing Hua University, Hsinchu 30013, Taiwan, Province of China

Received 8 October 2004; revised 28 December 2004; accepted 16 January 2005

Available online 7 April 2005

Abstract

Activation of hydrogen peroxide by different Cu(II)–amino acid complexes is performed and compared, with quinaldine blue as an oxidation indicator. Parameters such as pH and concentrations of Cu(II), hydrogen peroxide, and amino acids (L = glycine, alanine, and lysine) are examined to understand the activation mechanism of hydrogen peroxide. The experimental rate law determined is first order in Cu(II)–amino acid complexes and variable order in hydrogen peroxide, by Michaelis–Menten kinetics. It indicates that the formation of ligand–Cu(II)–peroxide complex may be responsible for the activation of hydrogen peroxide. The oxidation rate is also substantially enhanced in Cu(II)/amino acid/H_2O_2 systems with increasing pH from 6 to 9. The trend is consistent with the formation of hydroxyl radical ($^{\bullet}$OH), whose formation is favored in alkaline solutions. A mechanistic pathway that includes the formation of ligand–Cu(II)–peroxide complex and $^{\bullet}$OH is proposed. For glycine, alanine, and lysine, the maximum activation efficiencies appear at a ligand/copper molar ratio of 1.5–2.0, regardless of the change in pH values or ligand concentrations. According to the stability constants for Cu(II)–amino acid complexes, it is predicted that CuL and not CuL_2 is the dominant species forming the active copper complex catalyst.

Keywords: Copper complex; OH radical; Amino acid; Hydrogen peroxide; Quinaldine blue

1. Introduction

During the last decade activation of hydrogen peroxide by transition-metal ions, UV irradiation, and TiO_2 has received great attention for various applications [1–7]. Hydrogen peroxide (H_2O_2) is a common oxidizing agent and is often converted to hydroxyl radical ($^{\bullet}$OH) along with the redox reaction of transition-metal ions, that is, the Fenton or Fenton-like reaction. It has been reported that the activation of hydrogen peroxide in the presence of transition-metal ions is effective only under acidic conditions [8,9]. At higher pH, a major limitation is precipitation of the catalytically active metal ions. Nevertheless, these metal ions are relatively active when they are chelated as complexes in basic solutions [10,11]. The activation of hydrogen peroxide by transition-metal complexes has been widely applied to chemical synthesis, environmental control, effluent treatment, sterilization, etc. [12–17]. During a number of physiological processes, reactive oxygen species (ROS) contributed by the activation of hydrogen peroxide by iron or copper species are thought to be responsible for the oxidative modification of proteins and involved in aging and carcinogenesis [18–22]. Therefore, a better understanding of the reaction pathways in the activation of hydrogen peroxide and the oxidation of organic substrates is needed [23].

Recently, some studies have been carried out to investigate the Cu(II)/H_2O_2 reaction in the chemical mechanical planarization (CMP) process of integrated circuit (IC) industry [24–30]. Systems containing hydrogen peroxide as an oxidizer and Cu(II)(EDTA) or Cu(II)$(Glycine)_x$ as a catalyst have been successfully applied in the copper CMP of the IC industry. Fayolle and Romagna [24] reported that the use of hydrogen peroxide in CMP slurry produced better planarization results than $Fe(NO_3)_3$. Hariharaputhiran et

* Corresponding author.
E-mail address: chwu@mx.nthu.edu.tw (C.-H. Wu).

0021-9517/$ – see front matter
doi:10.1016/j.jcat.2005.01.038

al. [27] investigated the rate of copper removal by hydrogen peroxide in the presence of Cu(II)–glycine complexes. Their results demonstrated that the Cu(II)–glycine complex is an extremely effective catalyst in decomposing hydrogen peroxide to yield $^{\bullet}$OH, and, therefore, the dissolution and polish rates of copper block can be substantially enhanced. Zhang and Subramanian [28] found that the removal rates of copper were much more sensitive to the concentration of glycine than to that of hydrogen peroxide. Robbins and Drago [31] made a comparison of reaction rates with different complexing ligand systems and produced an experimental rate law. However, the detailed kinetics associated with each species were not thoroughly clarified in the previous studies, and little attention has been paid to the coordination effect of Cu(II) complexes.

Although several reaction mechanisms of metal ion species with hydrogen peroxide have been proposed, a paradigmatic mechanism has not been established. A mechanism, based on Haber–Weiss reaction or Fenton chemistry, assumed that metal ions were utilized through one-electron redox reactions that convert peroxide into reactive radical species [17,32,33]. It was claimed that the other mechanism included the formation of metal peroxo complexes (MOOH) as the early intermediates and no radical species were produced [33]. In the mechanism, the peroxide coordinated to the metal without changing its oxidation state, and the substrate might attack the coordinated and activated hydrogen peroxide. In many instances, the oxidation reaction is a combination of several mechanisms. To understand the activation mechanism of hydrogen peroxide followed by degradation of target substrates, a number of assays of radical species have been developed to distinguish radical chain processes from the others [34–36].

In this study, we attempt to characterize the effects of the composition of Cu(II)/amino acid/H_2O_2 reagent and pH on the activation of hydrogen peroxide, using quinaldine blue as an oxidation indicator. Systematic investigations are carried out to discuss the specific roles of Cu(II) speciation and the redox cycling of copper on the activation of hydrogen peroxide. A possible mechanism is proposed.

2. Experimental

2.1. Materials

All chemicals used were reagent grade or HPLC grade. L-Alanine (> 99.5%), L-glycine (> 99%), and L-lysine (> 99.5%) were obtained from Fluka (heavy metal impurities < 0.0005% m/m). H_3BO_3 (> 99.8%), *p*-nitrosodimethylaniline (PNDA) (> 98%), $CuCl_2 \cdot 2H_2O$ (> 99.0%), CuCl (> 99.0%), NaH_2PO_4 (> 99.5%), and hydroxylammonium chloride (> 99.0%) were obtained from Merck (Darmstadt, Germany). Quinaldine blue (1,1′-diethyl-2,2′-trimethinequinocyanine chloride; pinacyanol chloride), a redox indicator with a blue-purple color, was used as received from Aldrich. Hydrogen peroxide (30%) was obtained from Fluka and used after iodometric titration to verify its concentration. Other reagents used were NaCl (RDH, 99.8%), NaOH (J.T. Baker), HCl (J.T. Baker), acetonitrile (J.T. Baker), 2-nitrobenzaldehyde (98%, Aldrich), and bathocuproine (sulfonated sodium salt, GFS). All solutions were prepared with ultra-high-purity Milli-Q water exclusively ($\geqslant$ 18.2 MΩ cm resistivity; Millipore, Bedford, MA, USA). Solutions (or aliquots) were filtered through a 0.2-μm syringe filter (13 mm Teflon, or 25 mm Tuffryn; Acrodisc, Gelman). Glassware and quartzware were cleaned with a 50/50 v/v mixture of methanol and aqueous 3.0 M HCl and thoroughly rinsed with Milli-Q water. N_2 purging was used to remove O_2 from solutions to ensure an accurate measurement of Cu(I).

2.2. Visible spectrophotometry

Ultraviolet–visible absorbance measurements were made with a double-beam scanning spectrophotometer (Shimadzu UV-1601, Tokyo, Japan) and a custom-built constant-temperature (25 °C, Fisher 910 recirculator) variable-path-length aluminum cuvette holder (black-anodized). We obtained the oxidation rates of quinaldine blue by monitoring the absorbance change at 600 nm. We determined the consumption rates of PNDA by monitoring the absorbance change at 440 nm. Spectrophotometric determination of Cu(I) formed in the aqueous solution was performed with the bathocuproine method, which uses 2,9-dimethyl-4,7-diphenyl-1,10-phenanthrolinedisulfonic acid as the Cu(I) ligand, and we measured the absorbance of Cu(I) complex at 484 nm.

2.3. Preparation and procedures for kinetic study

Quinaldine blue is a cationic, basic dye with the structure shown in Scheme 1. Its absorbance maximum at 600 nm is insensitive to pH above pH 4. Simple UV–vis spectroscopic experiments are frequently used to monitor the amount of quinaldine blue decomposition, and investigations into its decomposing kinetics have been made to determine the activities of cytochrome c–crown ether complexes, manganese oxide catalysts, and related model catalysts [31,37–39]. For this study, we determined the oxidation rates of quinaldine blue by monitoring the decrease in its maximum absorbance at 600 nm. As the model compound, 0.006 g of quinaldine blue was dissolved in 100 ml of D.I. water as the stock solution and stored in the dark. The concentration was approx-

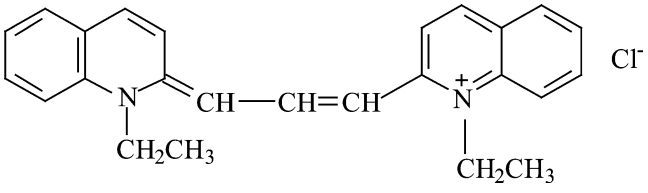

Scheme 1.

imately 1.6×10^{-4} M. The initial absorbance was checked before each experiment.

p-Nitrosodimethylaniline (PNDA) is a widely used •OH trapping reagent with a strong characteristic absorption peak at 440 nm. Upon the addition of •OH to the nitroso group of PNDA, the absorption at 440 nm is decreased significantly because the adduct of PNDA with •OH has a much weaker absorption at the same wavelength [Eq. (1)]. Since the reaction molar ratio of PNDA to •OH is 1:1, the formation of •OH can be determined by the consumption of PNDA. In each experiment, the initial concentration of PNDA was fixed at around 42 μM. The decrease in the concentration of PNDA is due solely to its consumption by the •OH generated in the solution, since the self-decomposition of PNDA is not significant above pH 5.8 [27,36,40].

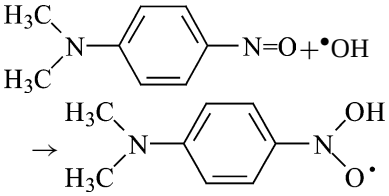

(1)

The following conditions were chosen for almost all of the kinetic studies for the oxidation experiment. A given sample solution was prepared in a 40 ml beaker with the addition of an aliquot of the hydrogen peroxide stock solution (0.88 M), Cu(II) stock solution (10.0 mM), or amino acid stock solution (10.0 mM) to a pre-made aqueous solution of quinaldine blue (2.0 ml stock solution) and 0.1 M borate buffer (10.0 ml). The mixture was diluted with D.I. water to a fixed volume of 30.0 ml. In each experiment, 3 ml of sample solution was withdrawn and then placed in a quartz cell (1.00-cm path length) while the UV measurement was processed. The initial rates of reaction were determined from data collected during the first 0.5 to 2.0 min of the reaction. The solution pH was measured with a Radiometer analytical Ioncheck 45 pH meter and combination glass electrode (Mettler Toledo Inlab 439/120). The pH of sample solutions was adjusted with the addition of aliquots of 1 or 0.1 M NaOH to the desired pH. The pH of the buffer was checked periodically and readjusted when necessary. In the experiment with •OH trapping, PNDA was added to each solution studied, with the same composition, except without quinaldine blue. To prevent the interference of formed gases, the sample solution (30 ml) was continuously stirred during the experiment. The stirring rate had a negligible effect on the oxidation rate of quinaldine blue.

3. Results and discussion

3.1. Kinetics of quinaldine blue oxidation

Fig. 1 shows the changes in the absorption spectra for quinaldine blue at different time intervals. These data clearly show how quinaldine blue is oxidized or decomposed as a function of time. Glycine was chosen as a model ligand in Cu(II) complexes because of its wide application in the copper CMP process. The result indicates that Cu(II), glycine, and H_2O_2 all together play important roles in quinaldine blue oxidation. Neither H_2O_2 nor Cu(II) complexes alone could oxidize quinaldine blue at the concentrations used in this work. Without ligand, only a small degree of quinaldine blue oxidizes in the Cu(II)/H_2O_2 system. After a period of incubation (10 min), the system color changed from purple to blackish green or brown instead of becoming colorless. A similar behavior was observed by Robbins and Drago, who proposed that copper precipitate forms in the absence of complexing reagent and the reaction is incomplete [29,31].

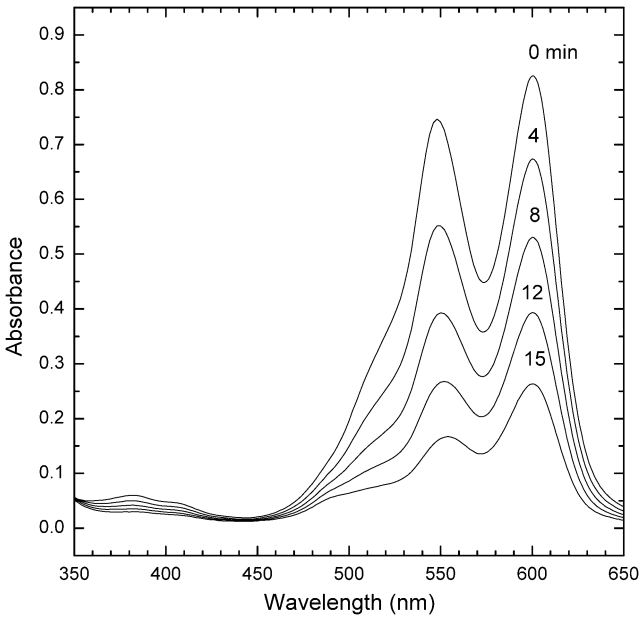

Fig. 1. UV/visible spectra of quinaldine blue for a solution containing 60 mM H_2O_2, 30 μM Cu(II), 0.24 mM glycine, and 0.033 M borate buffer at pH 7.5 as a function of time.

Table 1 lists the initial rates of quinaldine blue oxidation under specified conditions. Since all rate calculations involved initial rates at low conversions, the initial concentrations of Cu(II), glycine, and H_2O_2 could be regarded

Table 1
Dependence of quinaldine blue oxidation rate on quinaldine blue, Cu(II), glycine, and H_2O_2 concentrations[a]

[Quinaldine blue]	[Cu(II)]	[Glycine]	[H_2O_2]	Initial rate[b] (M min^{-1})	R^2
1.4×10^{-5}	3.0×10^{-5}	6.0×10^{-5}	3.2×10^{-2}	2.8×10^{-6}	1.00
9.0×10^{-6}	3.0×10^{-5}	6.0×10^{-5}	3.2×10^{-2}	2.8×10^{-6}	1.00
6.3×10^{-6}	3.0×10^{-5}	6.0×10^{-5}	3.2×10^{-2}	2.4×10^{-6}	1.00
9.0×10^{-6}	3.0×10^{-5}	1.6×10^{-4}	3.2×10^{-2}	8.1×10^{-7}	0.97
9.0×10^{-6}	3.2×10^{-4}	2.9×10^{-3}	4.5×10^{-2}	2.4×10^{-6}	1.00
9.0×10^{-6}	3.2×10^{-4}	2.9×10^{-3}	1.3×10^{-2}	1.1×10^{-6}	1.00
1.2×10^{-5}	3.2×10^{-4}	1.0×10^{-3}	4.5×10^{-2}	6.4×10^{-6}	0.99

[a] All concentrations are in M. All reaction solutions were in 0.033 M borate buffer at pH 8.2.

[b] The initial rate is calculated within one half-life.

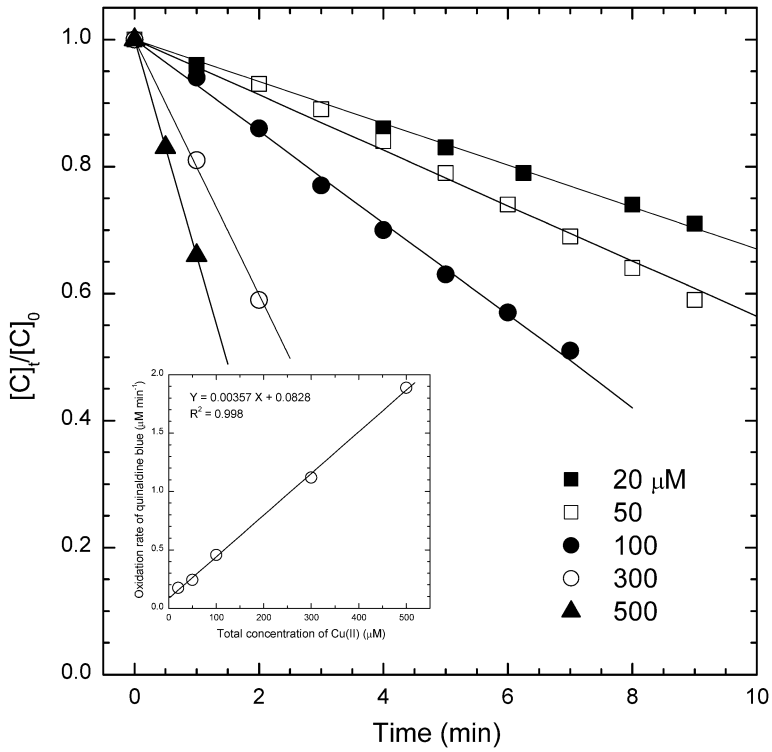

Fig. 2. Kinetic behavior of quinaldine blue oxidation versus time as a function of Cu(II) concentration in the presence of 40 mM H_2O_2, 5.0 mM glycine and 0.033 M borate buffer at pH 8.2. Numbers indicate the total concentration of Cu(II) concentration in μM. Inset: dependence of rate of quinaldine blue oxidation on the total concentration of Cu(II).

as constant values. Typically, the initial concentrations of H_2O_2 were kept in great excess over the concentrations of Cu(II) and quinaldine blue. Based on the data, the initial rates remained constant when the concentrations of quinaldine blue varied from 14 to 6.3 μM with 30 μM [Cu(II)], 60 μM [glycine], and 32 mM [H_2O_2] at pH 8.2 (shown in Table 1). Therefore, the reaction is zero order in quinaldine blue. Fig. 2 shows the kinetic plot of quinaldine blue oxidation in a Cu(II)/glycine/H_2O_2 system, where $[C]_t$ and $[C]_0$ refer to the concentrations of quinaldine blue at times t and zero, respectively. In the reaction of at least 50% conversion, good linearities ($R^2 > 0.97$) were obtained for the plots of $[C]_t/[C]_0$ versus time. When the reaction time exceeded one half-life, a slight deviation from zero-order kinetics was observed. This might result from the variation in hydrogen peroxide concentration. As shown in the inset of Fig. 2, the reaction rate displays a good linearity with [Cu(II)] under excess [glycine] and [H_2O_2]. This indicates that the reaction is first order in [Cu(II)].

The dependence of the reaction on H_2O_2 concentration is studied by measurement of the rate of the reaction at a different initial concentration of H_2O_2. These results indicate that the oxidation rate of quinaldine blue increases with increasing initial concentration of H_2O_2 but attains saturation at a high concentration of H_2O_2. The results are in contrast to the observations in Fig. 2. An inference from this saturation kinetics is that H_2O_2 binds to the catalyst, Cu(II)/glycine complex, before the oxidation of quinaldine blue. This phenomenon is similar to the enzyme catalytic reaction. Thus the kinetics of oxidation of quinaldine blue by the activation of hydrogen peroxide with Cu(II)/glycine complex as a catalyst can be analyzed in the form of the Michaelis–Menten equation [31,41–45]

$$rate = -\frac{\mathrm{d}[C]}{\mathrm{d}t} = \frac{V_{\max}[\mathrm{H_2O_2}]}{K_\mathrm{m} + [\mathrm{H_2O_2}]} \tag{2}$$

where *rate* (M/min) represents the velocity of oxidation of quinaldine blue, [C] (M) is the concentration of quinaldine blue, K_m (M) represents the affinity between the binding site of catalyst and H_2O_2, and $V_{\max}$ (M/min) represents the maximum catalytic reaction rate. From the inset of Fig. 2, $V_{\max}$ can be expressed as

$$V_{\max} = k_{\mathrm{cat}}[\mathrm{Cu(II)}]_T \tag{3}$$

where k_{cat} (min^{-1}) is the first-order rate constant. Inverting Eq. (2) and substituting Eq. (3) gives the reciprocal of the rate

$$\frac{[\mathrm{Cu(II)}]_T}{rate} = \frac{K_\mathrm{m}}{k_{\mathrm{cat}}[\mathrm{H_2O_2}]} + \frac{1}{k_{\mathrm{cat}}} \tag{4}$$

Eq. (4) is called the Lineweaver–Burk equation. Plotting $[\mathrm{Cu(II)}]_T/rate$ against $1/[\mathrm{H_2O_2}]$ gives an intercept of $1/k_{\mathrm{cat}}$ on the y axis as $1/[\mathrm{H_2O_2}]$ tends toward zero, and $1/[\mathrm{H_2O_2}] = -1/K_\mathrm{m}$ on the x axis. The slope of the line is $K_\mathrm{m}/k_{\mathrm{cat}}$. Fig. 3 shows the plot of $[\mathrm{Cu(II)}]_T/rate$ versus $1/[\mathrm{H_2O_2}]$, which reveals a good linear relationship. The results indicate that the activation of H_2O_2 catalyzed

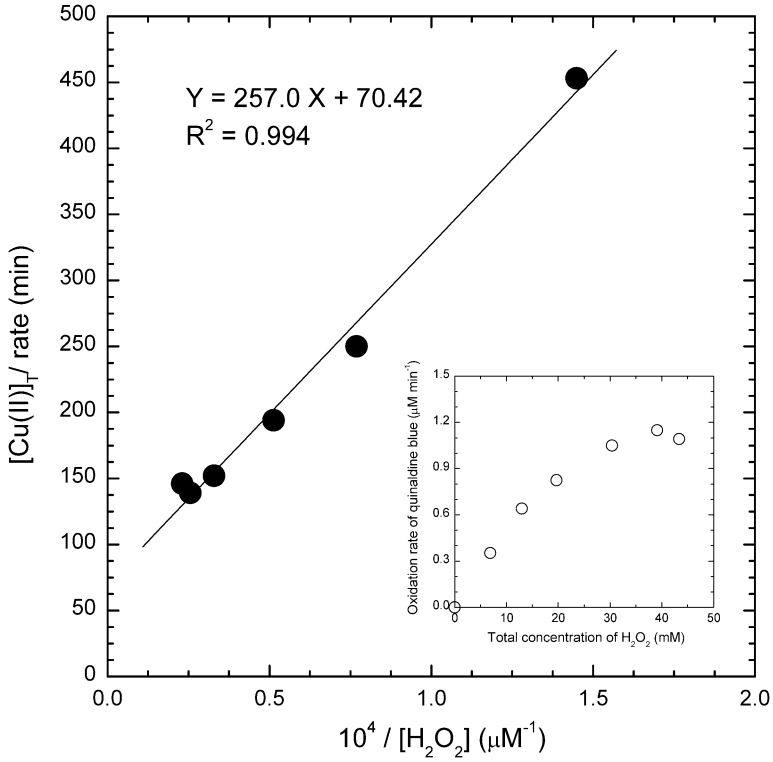

Fig. 3. [Cu(II)]/rate versus $[H_2O_2]^{-1}$ for the Cu(II)/glycine/H_2O_2 system. The mixtures consisted of 0.16 mM Cu(II), 2.86 mM glycine, and 0.033 M borate buffer at pH 8.2. Inset: raw kinetic data.

by Cu(II)/glycine complex follows the Michaelis–Menten mechanism. When $[H_2O_2]$ is much higher than K_m, the rate reaches V_{max}, and the zero-order rate occurs. Therefore, when $[H_2O_2]$ is in excess, k_{cat} shows the oxidation rate of quinaldine blue in unit concentration of Cu(II)/glycine complex, which is also the catalytic activity per molecule of the complex on the activation of H_2O_2 to more reactive oxygen species. We proposed a more detailed mechanism by showing that the coordination of hydroperoxide anion with copper complexes might produce the peroxo or hydroperoxo complexes and directly or indirectly induce the oxidation of organics [33].

3.2. pH effect

Fig. 4 shows the plots of oxidation rate of quinaldine blue and the formation rate of •OH versus pH. The oxidation rate increased exponentially as the pH was varied from 6.0 to 8.5. As shown in Fig. 4, the oxidation rate of quinaldine blue correlates markedly with the formation rate of •OH. The trend is consistent with the formation of •OH, the formation of which is favored under alkaline conditions [5,33,45]. Fig. 5 shows the formation of Cu(I) concentration versus time in different Cu(II)/H_2O_2 systems. As can be seen, Cu(I) was detected and accumulated in the deaerated systems. The formation of Cu(I) depends on the concentration of H_2O_2 and that of alanine. The formation of Cu(I) leveled off at higher concentration when the initial concentration of H_2O_2 was higher in the system without amino acids. Meanwhile,

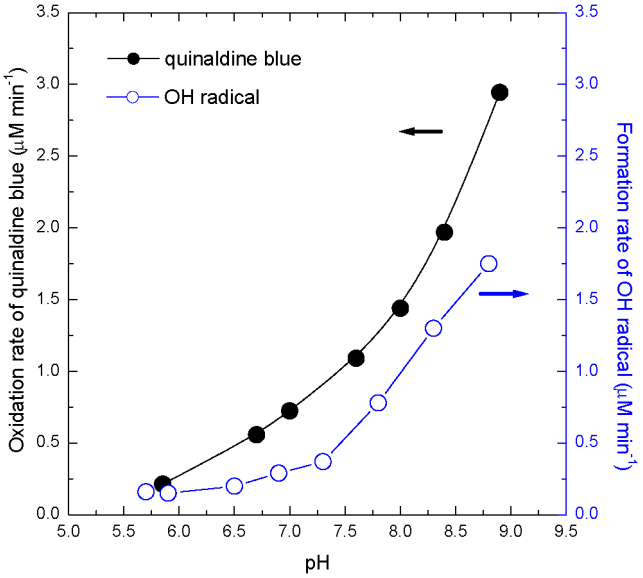

Fig. 4. Effect of pH on the reaction rate for quinaldine blue oxidation and hydroxyl radical formation in the condition of 0.32 mM Cu(II), 2.86 mM glycine, 43.4 mM H_2O_2, and 0.033 M borate buffer. The initial absorbances of quinaldine blue at 600 nm and PNDA at 440 nm were 0.60 and 0.80, respectively.

alanine, a strong complexing agent for Cu(II), could accelerate the redox cycling of the Cu(II)/Cu(I) reaction because a higher Cu(I) concentration was measured in the alanine-added system. Therefore, the reduction reaction of Cu(II) complexes should be involved in the activation of hydrogen

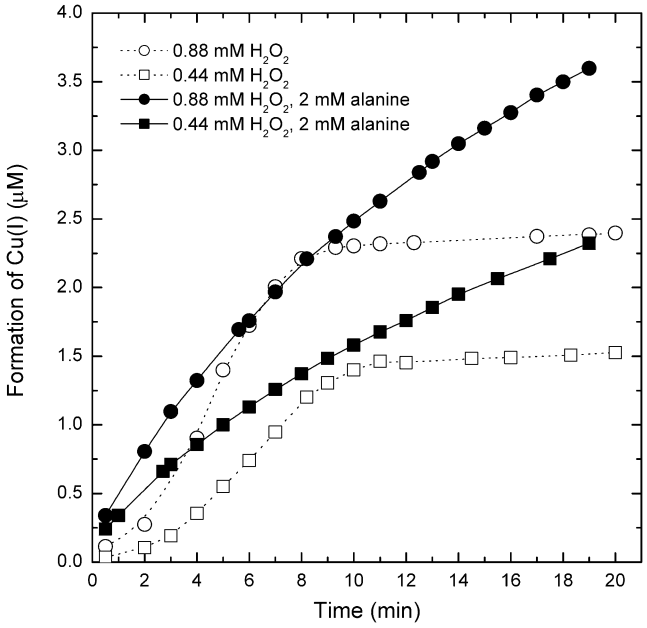

Fig. 5. Plot of formation of Cu(I) versus time at different concentrations of H_2O_2 and alanine. The mixtures consisted of 0.20 mM Cu(II), 100 μM phosphate buffer, and 0.10 M NaCl at pH 7.4.

peroxide to form •OH. The results indicate that not only is the oxidation rate of quinaldine blue correlated with •OH, but the formation pathway of •OH might also accompany the redox cycling of copper. Based on the results of previous studies, the system might produce •OH, according to the following Fenton or Fenton-like reactions:

$$\text{L–Cu}^{2+} + \text{H}_2\text{O}_2 \rightarrow \text{L–Cu} \cdot \text{OOH}^{+} + \text{H}^{+} \quad (5)$$

$$\text{L–Cu} \cdot \text{OOH}^{+} \rightarrow \text{L–Cu}^{+} + \text{HO}_2^{\bullet} \quad (6)$$

$$\text{L–Cu}^{2+} + \text{H}_2\text{O}_2 \rightarrow \text{L–Cu}^{+} + \text{HO}_2^{\bullet} + \text{H}^{+} \quad (7)$$

$$\text{L–Cu}^{+} + \text{H}_2\text{O}_2 \rightarrow \text{L–Cu}^{2+} + \text{OH}^{-} + {}^{\bullet}\text{OH} \quad (8)$$

Shah et al. investigated the possibility that different types of radicals are simultaneously formed in the system [2]. From the ESR spectra of spin adducts of 5,5′-dimethyl-1-pyrroline N-oxide (DMPO), they observed that the •OH behaved slightly differently in a magnetic field, which indicates that the radicals could not only diffuse into the solutions but also bind with the ligand to form ligand–Cu(II)–radical complexes. As shown in Fig. 4, which compares the oxidation rate of quinaldine blue (r_{QB}) with the formation rate of •OH (r_{PNDA}), the ratio of r_{QB} to r_{PNDA} is larger than 1.0 and changes with the variation in pH. This implies that in addition to •OH-dependent reactions, ligand–Cu(II)–radical complexes may also be responsible for the oxidation of quinaldine blue [1,33,46]. This phenomenon is similar to the case of aqueous phase photoformation of •OH in the cloud waters, which is apportioned into two categories: H_2O_2-dependent and H_2O_2-independent sources [47]. Ali et al. [48] showed that the metal-catalyzed oxidation process with Cu(II) under different oxidation conditions had a larger impact than Cu(I). They suggested that the conversion of Cu(II) to Cu(I) could result in extra oxidative steps in addition to the Fenton reaction of Cu(I) with H_2O_2.

3.3. Effect of the molar ratio of glycine/Cu(II)

The effect of Cu(II)/amino acid complexes on the oxidation rate of quinaldine blue was investigated. For this purpose, various ligands with different concentrations were added to the system. Under the system conditions of 30 μM Cu(II) and 6.0 mM H_2O_2, the reaction rate reaches its maximum when the molar ratio of glycine to Cu(II) ions is around 2.0. However, the reaction rate decreases dramatically when the ratio is above 3.0. The trend shows no significant change, even when the concentration of Cu(II) or H_2O_2 increases by up to 10-fold. As shown in Fig. 6, similar results were observed with the variation of pH values.

Although complexes with different ligand coordination might have quite different catalytic abilities, the effect of copper speciation has not been investigated in detail [2,27,31]. In this study, the distribution of Cu(II) species such as 1:1 or 1:2 Cu(II) to glycine complex (CuL, CuL_2), inorganic free copper ions (Cu_{in}), etc. under each experimental condition was calculated with the WIN MINTEQ computer program with critically reviewed thermodynamic equilibrium constants [49,50]. Table 2 shows the molar fraction of copper–glycine complex and its relative oxidation rate of quinaldine blue with different pH values and glycine concentrations. The results show that Cu(II)–glycine complex is the major species correlated with the enhancement

Table 2
Distribution of copper species in different experimental conditions and their catalytic abilities relative to the oxidation of quinaldine blue[a,b]

[Glycine]	$f_{Cu,in}$	$f_{Cu(gly)}$	$f_{Cu(gly)2}$[c]	Rate[d]
		pH = 6.5		
30	0.41	0.55	0.04	0.13
45	0.26	0.65	0.09	0.19
60	0.18	0.68	0.14	0.16
75	0.13	0.67	0.20	1.14
90	0.09	0.66	0.25	0.13
		pH = 7.5		
30	0.37	0.47	0.16	1.5
40	0.24	0.50	0.26	3.5
50	0.16	0.48	0.36	2.5
60	0.10	0.44	0.46	1.8
70	0.09	0.39	0.52	1.0
90	0.04	0.30	0.66	0.54
		pH = 8.2		
32	0.46	0.23	0.31	9.6
53	0.21	0.21	0.58	13.6
60	0.22	0.18	0.60	8.3
80	0.04	0.10	0.86	1.9
90	0.02	0.08	0.90	1.0

[a] All concentrations are in μM.
[b] [Cu(II)] = 30 μM, [H_2O_2] = 6.0 mM, borate buffer = 0.033 M.
[c] f, the equilibrium fraction of the total copper present as the ith complex. The subscript "in" represents all forms of inorganic Cu(II).
[d] The rate is expressed in μM min^{-1}.

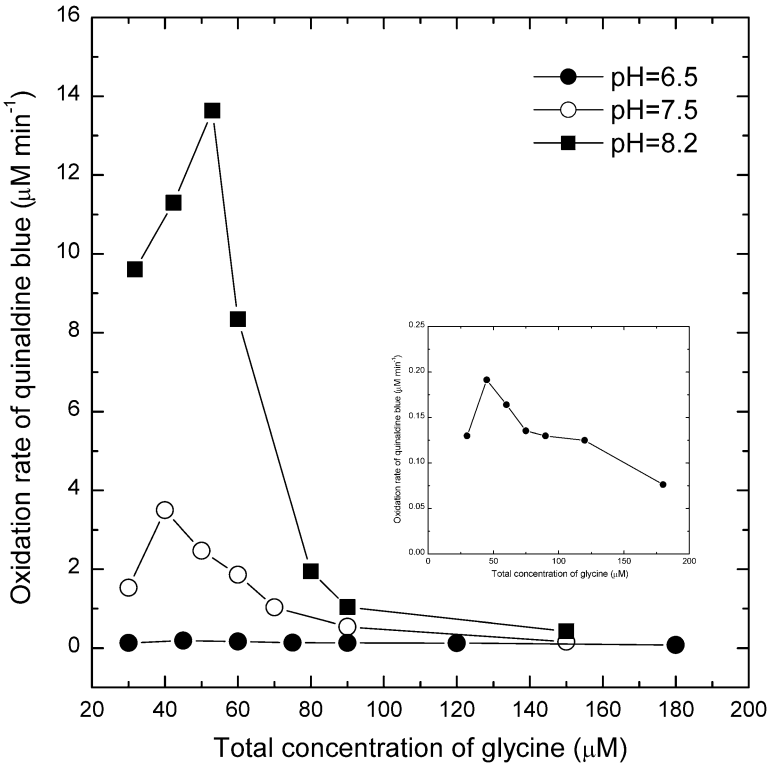

Fig. 6. Effect of glycine concentration on the oxidation rate of quinaldine blue as a function of pH. The system was controlled under the condition of 30 μM Cu(II), 6.0 mM H_2O_2, and 0.033 M borate buffer solution. The initial absorbance of quinaldine blue at 600 nm was 0.80. Inset: effect of glycine concentration on the reaction rate of quinaldine blue oxidation at pH 6.5.

of reaction rate in the catalytic system. When the system achieved its maximum reaction rate, above 75% of Cu(II) formed complexes with ligands. Meanwhile, the level of major Cu(II)-complex species could not be inferred simply from the molar ratio of ligand to Cu(II) ions. Taking the condition of pH 6.5, for example, when the molar ratio of glycine to Cu(II) is 2.0, the major species is 1:1 Cu(II) to glycine complex (CuL ∼ 68%), not 1:2 Cu(II) to glycine complex (CuL_2). Moreover, precipitation of Cu(II) species may form in the high-pH condition (> 6.5) when the system molar ratio of glycine to Cu(II) is below 1.3, which indicates that the copper precipitates have a lower catalytic activity than CuL.

In addition to glycine, two other amino acids (lysine and alanine) were studied in the oxidation of quinaldine blue. Fig. 7 shows that the maximum oxidation rate could be found at the ligand/Cu(II) molar ratio point of 1.5–2.0. Compared with the modeling data for species analysis, the trend of the reaction rate is consistent with the fraction of CuL. Among the copper complexing agents tested in the experiments, alanine exhibits the highest catalytic activity. The activities of catalyzing hydrogen peroxide are followed in this order: alanine > lysine > glycine. Ligand structure influences the stability constants of copper complexes and may result in different physiochemical properties. It has been shown that the structure of organic Cu(II) complexes, which correlates with the relative stability of the carbon-centered radicals and the efficiency of the initial photoinduced ligand-to-metal electron transfer, has a strong impact on the quantum yield of photolysis of Cu(II)/dicarboxylate complexes [51,52]. The kinetics of the photolysis of Cu(II)/amino acid complexes were investigated under irradiation at 313 nm [53]. In the photochemical study, the Cu(I) quantum yield for the Cu(II)-β-alanine complex was higher than those for amino acid systems, including aspartic acid, glutamic acid, glycine, and histidine. The photocatalyzed mineralization of amino acids at the titania/water interface has been investigated [54]. The yield of ammonium ion for alanine was higher than those for serine and phenylalanine. These results are consistent with the observation in the current study. To elucidate the effects of ligand structure on the activation of hydrogen peroxide, further studies of the catalytic properties of Cu(II) complexes with different amino acids are needed.

3.4. Proposed mechanism

Based on the results of this work and on the literature [2,18,19,23,31,33,42–46], a possible mechanistic pathway for the oxidation of quinaldine blue with hydrogen peroxide as oxidant and copper complex as catalyst is depicted in Fig. 8. The Cu(II) ion is found to be sixfold coordinated with four equatorial and two axial ligands and exhibits a distorted octahedral structure. The high lability of hydrated Cu(II) ion is attributed to the dynamic Jahn–Teller effect [55,56]. Normally, the water exchange rate constant (k) for solvated

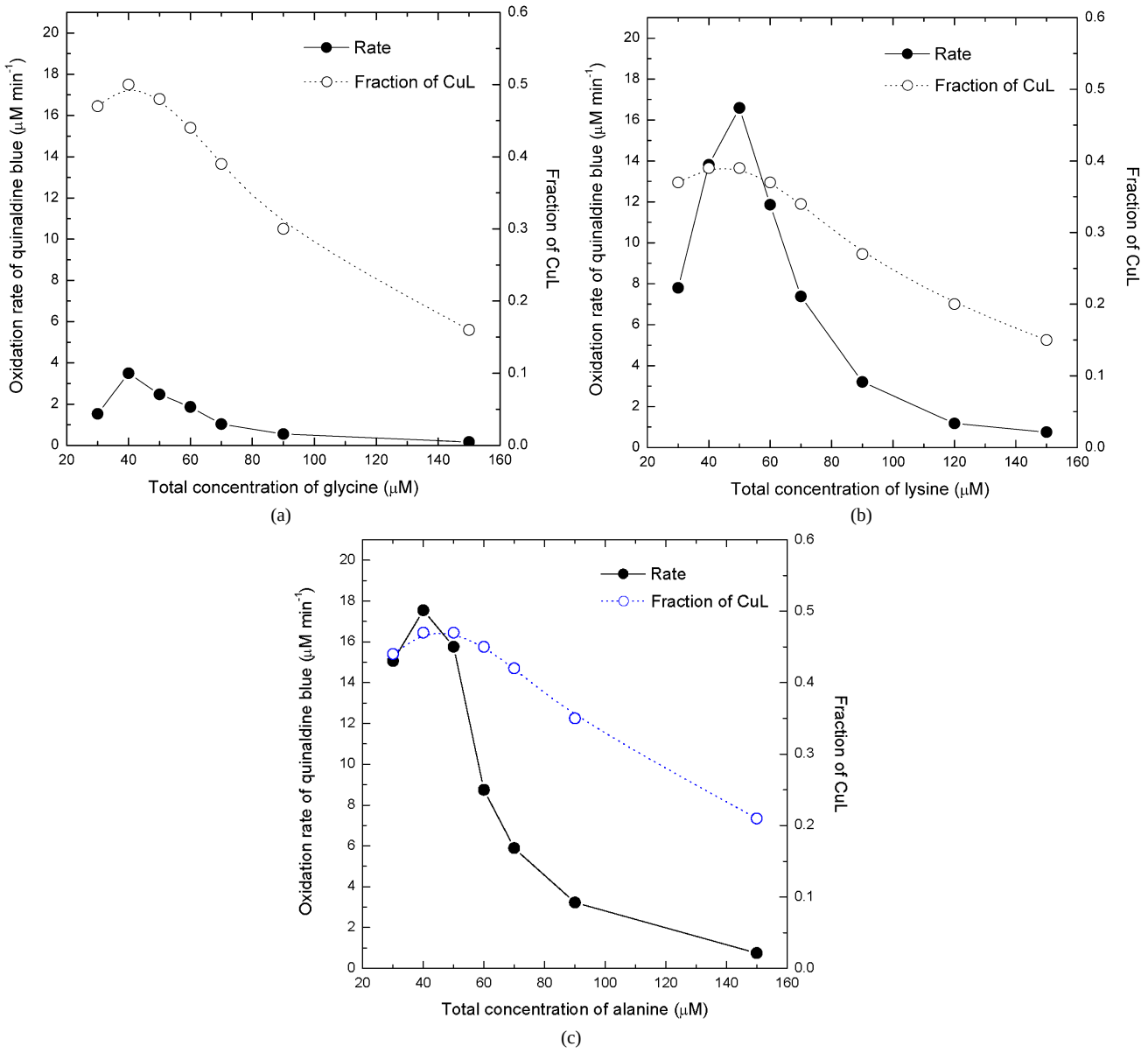

Fig. 7. Dependence of oxidation rate of quinaldine blue on the molar ratio of amino acid to Cu(II). The system was controlled under the condition of 30 μM Cu(II), 6.0 mM H_2O_2, and 33 mM borate buffer solution at pH 7.5. The initial absorbance of quinaldine blue at 600 nm was 0.80. (a) Glycine, (b) lysine, (c) alanine.

Cu(II) at 298 K is very fast (4.4×10^9 s^{-1}), and the lifetime of the complex is in the picosecond time scale, with an activation energy of 3.5 kJ mol^{-1} [55]. Therefore, as shown in Fig. 8, the reversible dissociation of a water molecule from a distorted octahedral Cu(II) complex is reasonably easy. Then, coordination of the hydroperoxide anion (O_2H^-) with Cu(II) complex may produce the peroxo or hydroperoxide complex. Once formed, the copper–hydroperoxo species or other ROS formed from the intermediates may react extremely rapidly with quinaldine blue. Simultaneously, Cu(II) complex may react directly with hydrogen peroxide and induce electron transfer from hydrogen peroxide to Cu(II), and subsequently redox cycling of copper proceeds. When the back electron transfer of Cu(I) complexes occurs, hydrogen peroxide may dissociate to $^{\bullet}OH$. As a result, the active $^{\bullet}OH$ reacts rapidly with the substrate. Therefore, pathways proposed for the formation of $^{\bullet}OH$ and ligand–Cu(II)–peroxide complexes may both be responsible for the oxidation of quinaldine blue in the Cu(II)/amino acid/H_2O_2 system. Useful information can be provided by the variation of Cu(II), complexing ligands, pH, solvent composition, and target substrates. The oxidation rate of quinaldine blue can be greatly enhanced in alkaline environments because of the favorable formation of reactive species, especially for hydroperoxo complex. The formation of stable hydroperoxo complex is necessary to have two equatorial coordination sites occupied by easily displaced solvent. In this study, the hydroperoxo complex may form when one wa-

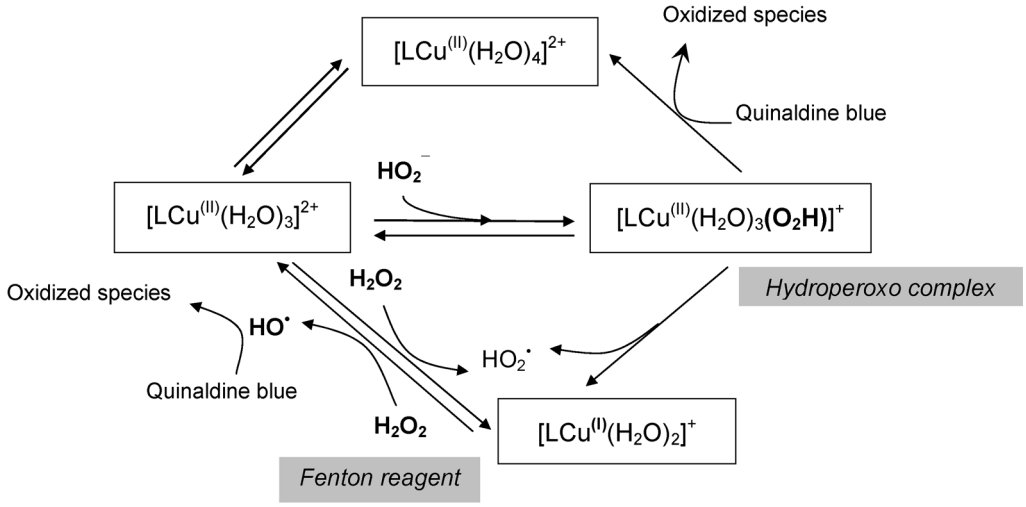

Fig. 8. Proposed mechanism for the hydrogen peroxide activation by Cu(II).

ter is dissociated from the axial positions of Cu(II) complex followed by the attack and binding of HO_2^- at its equatorial positions [31]. Therefore, it is reasonable to expect that the peak oxidation rate of quinaldine blue always occurs as CuL complex is the main species in the system. When the CuL_2 complex is formed, the oxidation rate decreases as predicted because there are no strongly binding equatorial positions available to bind the HO_2^-. Furthermore, the oxidation rate may be suppressed with excess noncoordinated glycine (glycine/Cu(II) > 5). Further studies on the analysis of $^\bullet$OH or other formed by-products could provide an explanation for why the reaction rates are so sensitive to the variation in glycine concentration.

4. Conclusions

The catalytic activity of copper complexes on hydrogen peroxide has been evaluated by examination of the oxidation rate of quinaldine blue. The formation of $^\bullet$OH and ligand–Cu(II)–peroxide complex favors contribution to the oxidation of quinaldine blue, implying that at least two pathways may be responsible for the activation of hydrogen peroxide. The observed kinetic data and speciation analysis show that 1:1 Cu(II)–ligand complex (CuL) is the dominant species forming the active copper complex catalyst. A possible mechanistic pathway for the activation of hydrogen peroxide is proposed.

Acknowledgment

This work was supported by the National Science Council of the Republic of China (Taiwan) under grant no. NSC-92-2113-M-007-063.

References

[1] R. Cai, Y. Kubota, A. Fujishima, J. Catal. 219 (2003) 214.
[2] V. Shah, P. Verma, P. Stopka, J. Gabriel, P. Baldrian, F. Nerud, Appl. Catal. B: Environ. 46 (2003) 287.
[3] M. Akagawa, K. Suyama, Free Radic. Res. 36 (2002) 13.
[4] I.A. Salem, Chemosphere 44 (2001) 1109.
[5] P. Verma, V. Shah, P. Baldrian, J. Gabriel, P. Stopka, T. Trnka, F. Nerud, Chemosphere 54 (2004) 291.
[6] P. Verma, P. Baldrian, F. Nerud, Chemosphere 50 (2003) 975.
[7] F. Nerud, P. Baldrian, J. Gabriel, D. Ogbeifun, Chemosphere 44 (2001) 957.
[8] X.-K. Zhao, G.-P. Yang, Y.-J. Wang, X.-C. Gao, J. Photochem. Photobiol. A: Chem. 161 (2004) 215.
[9] J. Feng, X. Hu, P.L. Yue, Chem. Eng. J. 100 (2004) 159.
[10] A. El-Jammal, D.M. Templeton, Inorg. Chim. Acta 245 (1996) 199.
[11] S. Hanaoka, J.M. Lin, M. Yamada, Anal. Chim. Acta 409 (2000) 65.
[12] V. Conte, F.D. Furia, G. Licini, Appl. Catal. A: Gen. 157 (1997) 335.
[13] A.P. Deshmukh, V.G. Akerkar, M.M. Salunkhe, J. Mol. Catal. A: Chem. 153 (2000) 75.
[14] S. Velusamy, T. Punniyamurthy, Tetrahedron Lett. 44 (2003) 8955.
[15] H.H. Monfared, Z. Amouei, J. Mol. Catal. A: Chem. 217 (2004) 161.
[16] T. Pacześniak, A. Sobkowiak, J. Mol. Catal. A: Chem. 194 (2003) 1.
[17] H.B. Dunford, Coord. Chem. Rev. 233–234 (2002) 311.
[18] A.M. Mohamadin, J. Inorg. Biochem. 84 (2001) 97.
[19] D. Bar-Or, L.T. Rael, E.P. Lau, N.K.R. Rao, G.W. Thomas, J.V. Winkler, R.L. Yukl, R.G. Kingston, C.G. Curtis, Biochem. Biophys. Res. Commun. 284 (2001) 856.
[20] J. Ueda, K. Anzai, Y. Miura, T. Ozawa, J. Inorg. Biochem. 76 (1999) 55.
[21] J. Ueda, M. Takai, Y. Shimazu, T. Ozawa, Arch. Biochem. Biophys. 357 (1998) 231.
[22] E.R. Stadtman, Free Rad. Biol. Med. 9 (1990) 315.
[23] J.F. Perez-Benito, J. Inorg. Biochem. 98 (2004) 430.
[24] M. Fayolle, F. Romagna, Microelectron. Eng. 37 (1997) 135.
[25] T. Du, Y. Luo, V. Desai, Microelectron. Eng. 71 (2004) 90.
[26] Y. Ein-Eli, E. Abelev, D. Starosvetsky, Electrochim. Acta 49 (2004) 1499.
[27] M. Hariharaputhiran, J. Zhang, S. Ramarajan, J.J. Keleher, Y. Li, S.V. Babu, J. Electrochem. Soc. 147 (2000) 3820.
[28] L. Zhang, R.S. Subramanian, Thin Solid Films 397 (2001) 143.
[29] S. Aksu, L. Wang, F.M. Doyle, J. Electrochem. Soc. 150 (2003) G718.
[30] S. Seal, S.C. Kuiry, B. Heinmen, Thin Solid Films 423 (2003) 243.
[31] M.H. Robbins, R.S. Drago, J. Catal. 170 (1997) 295.
[32] C.C. Winterbourn, Toxicol. Lett. 82/83 (1995) 969.

[33] R.S. Drago, Coord. Chem. Rev. 117 (1992) 185.
[34] Y. Du, J. Rabani, J. Phys. Chem. B 107 (2003) 11970.
[35] L. Sun, J.R. Bolton, J. Phys. Chem. 100 (1996) 4127.
[36] J. Keleher, J. Zhang, S. Waud, Y. Li, Chem. Educator 5 (2000) 242.
[37] S.R. Segal, S.L. Suib, L. Foland, Chem. Mater. 9 (1997) 2526.
[38] T. Yamada, K. Kikawa, S. Shinoda, H. Tsukube, Tetrahedron Lett. 40 (1999) 6967.
[39] T. Yamada, S. Shinoda, K. Kikawa, A. Ichimura, J. Teraoka, T. Takui, H. Tsukube, Inorg. Chem. 39 (2000) 3049.
[40] L. Zang, P. Qu, J. Zhao, T. Shen, H. Hidaka, J. Mol. Catal. A: Chem. 120 (1997) 235.
[41] X.L. Chen, D.H. Li, H.H. Yang, Q.Z. Zhu, H. Zheng, J.G. Xu, Anal. Chim. Acta 434 (2001) 51.
[42] V.K. Sivasubramanian, M. Ganesan, S. Rajagopal, R. Ramaraj, J. Org. Chem. 67 (2002) 1506.
[43] L.H. Chen, L.Z. Liu, H.X. Shen, Anal. Chim. Acta 480 (2003) 143.
[44] K. Selmeczi, M. Reglier, M. Giorgi, G. Speier, Coord. Chem. Rev. 245 (2003) 191.
[45] Y. Huang, J. Li, W. Ma, M. Cheng, J. Zhao, J.C. Yu, J. Phys. Chem. B 108 (2004) 7263.
[46] P. Chen, K. Fujisawa, E.I. Solomon, J. Am. Chem. Soc. 122 (2000) 10177.
[47] T. Arakaki, B.C. Faust, J. Geophys. Res. 103 (1998) 3487.
[48] F.E. Ali, K.J. Barnham, C.J. Barrow, F. Separovic, J. Inorg. Biochem. 98 (2004) 173.
[49] A.E. Martell, R.M. Smith, R.J. Motekaitis, NIST Critically Selected Stability Constants of Metal Complexes, Version 7.0, NIST Standard Reference Database 46 (2003).
[50] J.D. Allison, D.S. Brown, K.J. Novo-Gradac, MINTEQA2/PRODEFA2, A Geochemical Assessment Model for Environmental Systems: Version 4.0 (EPA/600/3-91/021); US Environmental Protection Agency, Athens, GA (1999).
[51] L. Sun, C.-H. Wu, B.C. Faust, J. Phys. Chem. A 102 (1998) 8664.
[52] C.-H. Wu, L. Sun, B.C. Faust, J. Phys. Chem. A 104 (2000) 4989.
[53] K. Hayase, R.G. Zepp, Environ. Sci. Technol. 25 (1991) 1273.
[54] S. Horikoshi, N. Serpone, J. Zhao, H. Hidaka, J. Photochem. Photobiol. A: Chem. 118 (1998) 123.
[55] D.H. Powell, L. Helm, A.E. Merbach, J. Chem. Phys. 95 (1991) 9258.
[56] C.F. Schwenk, B.M. Rode, Chem. Phys. Chem. 4 (2003) 931.